Nuclear Engineering and Technology 49 (2017) 769–775

Contents lists available at ScienceDirect

Nuclear Engineering and Technology

journal homepage: www.elsevier.com/locate/net

Original Article

Corrosion behavior induced by LiCl-KCl in type 304 and 316 stainless steel and copper at low temperature

Jee-Hyung Sim [a, *], Yong-Soo Kim [a], Il-Je Cho [a, b]

[a] Department of Nuclear Engineering, Hanyang University, 222 Wangsimni-ro, Seongdong-gu, Seoul, 04763, Republic of Korea
[b] Korea Atomic Energy Research Institute, 1045 Daedeok-daero, Yuseong-gu, Daejeon, 34057, Republic of Korea

ARTICLE INFO

Article history:
Received 19 October 2016
Received in revised form
9 February 2017
Accepted 18 February 2017
Available online 10 March 2017

Keywords:
Copper
Pitting Corrosion
Pyroprocessing
Stainless Steel

ABSTRACT

The corrosion behavior of stainless steel (304 and 316 type) and copper induced by LiCl-KCl at low temperatures in the presence of sufficient oxygen and moisture was investigated through a series of experiments (at 30°C, 40°C, 60°C, and 80°C for 24 hours, 48 hours, 72 hours, and 96 hours). The specimens not coated on one side with an aqueous solution saturated with LiCl-KCl experienced no corrosion at any temperature, not even when the test duration exceeded 96 hours. Stainless steel exposed to LiCl-KCl experienced almost no corrosion below 40°C, but pitting corrosion was observed at temperatures above 60°C. As the duration of the experiment was increased, the rate of corrosion accelerated in proportion to the temperature. The 316 type stainless steel exhibited better corrosion resistance than did the 304 type. In the case of copper, the rate of corrosion accelerated in proportion to the duration and temperature but, unlike the case of stainless steel, the corrosion was more general. As a result, the extent of copper corrosion was about three times that of stainless steel.

1. Introduction

The ever increasing demand for energy and for lower carbon emissions has created a greater focus on the role of nuclear energy in providing an alternative energy source, but there are still concerns over how to deal with spent nuclear fuel, which still contains considerable amounts of nuclear materials even after it is discharged from the nuclear plant [1]. Pyroprocessing is one of the more promising methods for treating spent nuclear fuel, as this technique can recover uranium and transuranic elements, thereby increasing uranic resource utilization efficiency while also reducing the amount of highly radioactive waste. This, in turn, can increase the efficiency of disposal facilities and reduce the disposal period. Moreover, by recovering transuranic elements (TRUs) collectively rather than separately, this method can help prevent nuclear proliferation. This has led to numerous studies being conducted both domestically and internationally [2–4].

To verify the technical validity of pyroprocessing and to produce reliable scale-up data, the PyRoprocess Inactive DEmonstration facility (PRIDE) was constructed and operated at the Korea Atomic Energy Research Institute (KAERI). This experimental facility is dedicated to an engineering-scale pyroprocess, with most equipment being operated under an environment of high-temperature molten salt [5,6]. As the major structural materials inside the facility are therefore used under conditions that are mechanically and chemically harsh, any reactions or changes are very important in that they can directly affect the stability of the entire facility. Numerous experiments have been conducted on the stainless steel and copper used as the main structural materials at PRIDE; in these experiments, it has been found that chloride ions have the greatest influence on the corrosion rate [7–14].

It is well known that stainless steel experiences almost no corrosion in environments without oxygen and moisture; however, as indicated in the experiments of Pettersson et al [15], this material suffers from an accelerated rate of corrosion with time and temperature when exposed to oxygen and moisture at temperatures above 400°C. When exposed to chloride, the rate of corrosion is further accelerated, particularly at higher temperatures. Like that of stainless steel, the corrosion rate of copper is accelerated in a medium that contains chloride [16,17], and for this reason, the inside of PRIDE is filled with high-purity argon gas to maintain low concentrations (a few ppm) of oxygen and moisture. However, as there is currently insufficient experimental data for the low temperature (< 100°C) conditions found inside PRIDE, corrosion

* Corresponding author.
E-mail address: shimnara@hanyang.ac.kr (J.-H. Sim).

http://dx.doi.org/10.1016/j.net.2017.02.007

Table 1
Chemical compositions of stainless steels tested (wt.%).

	C	Si	Mn	P	S	Ni	Cr	Mo
304SS	0.08	1.0	2.0	0.045	0.03	8	18	–
316SS	0.08	1.0	2.0	0.04	0.03	12	17	2–3

experiments were conducted on the major structural materials (304 and 316 stainless steel, and copper). This research also considered abnormal conditions under which the oxygen and moisture excessively increase at a temperature similar to that inside PRIDE. During these corrosion experiments, time and temperature were set as variables, and gravimetric analysis was performed to measure the rate of corrosion. In addition, by conducting a component analysis and surface analysis of the corrosion product, the corrosion behavior induced by LiCl-KCl was evaluated.

2. Materials and methods

2.1. Specimen preparation

Coin-shaped specimens of the major structural materials of PRIDE (304SS, 316SS and copper) were manufactured to a diameter of 2.5 cm and thickness of 2 mm from plates of each material. The chemical compositions of the two stainless steels are shown in Table 1. The surface of each specimen was ground using 1,000-grit SiC paper, polished with colloidal silica to a mirror finish, and then washed in acetone and ethanol. An ultrasonic cleaner was used to remove any debris from the surface, after which the samples were stored in a desiccator to prevent any surface oxidation. After weighing each specimen to the nearest 10 μg, a micropipette was used to apply a saturated LiCl-KCl aqueous solution over their entire upper surface in preparation for corrosion testing. The samples were reweighed after testing to determine the rate of corrosion.

2.2. Corrosion rate measurement

Corrosion experiments were conducted in a quartz tube with an inner diameter of 50 mm; an electric furnace was used to maintain a constant temperature inside the tube (Fig. 1). To ensure a corrosive environment, the injection of oxygen from the outside was controlled, and distilled water was added to the bottom of the sealed quartz tube to maintain saturated water vapor pressure. Specimens of each of the three materials were mounted onto an alumina holder, which was then inserted into the chamber. To evaluate the change in corrosion behavior with temperature and time, experiments were conducted at 30°C, 40°C, 60°C, and 80°C for 24 hours, 48 hours, 72 hours, and 96 hours. Each specimen undergoing the corrosion progress was subjected to surface and component analysis by Scanning Electron Microscopy (SEM), Auger Electron Spectroscopy (AES), and X-ray Photoelectron Spectroscopy (XPS). These analyses were carried out using Nova Nano SEM (SEM) from FEI-Co., PHI700Xi (AES) from Physical Electronics, and Theta probe system (XPS) from Thermo-Fisher Scientific Co. To provide a reference, the same experiments were conducted on specimens not coated with LiCl-KCl solution, but no corrosion was observed.

3. Results and discussion

3.1. Gravimetry

The corrosion product formed on each of the specimens was removed in accordance with KS D ISO 8407, and the weight loss of each specimen was measured [18]. The weight change after

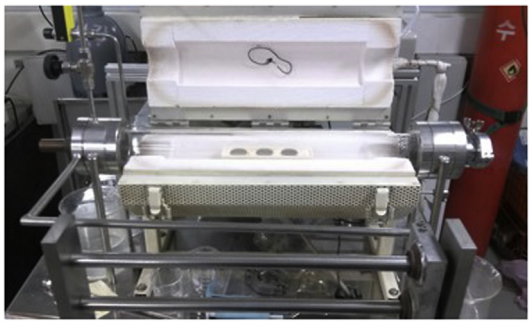

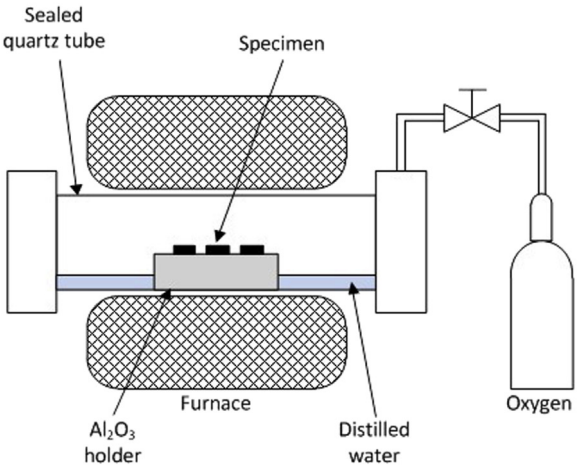

Fig. 1. Apparatus used for corrosion experiments.

corrosion should be > 100 μg for the test to be considered valid, but the two stainless steels lost only a few tens of μg below 40°C, even after 96 hours. As such, their weight loss could not be calculated. However, the weight loss quickly increased with time at temperatures above 60°C, as shown in Fig. 2. Given that the specimens not coated with LiCl-KCl did not corrode, it can be inferred that the presence of chloride ions greatly accelerates the corrosion of stainless steel, especially at high temperatures. In the case of 304SS, the difference in weight loss between the two temperatures of 60°C and 80°C was a meager 0.01 mg/cm^2 after 24 hours, but this increased to 0.04 mg/cm^2, 0.1 mg/cm^2, and 0.18 mg/cm^2 after 48

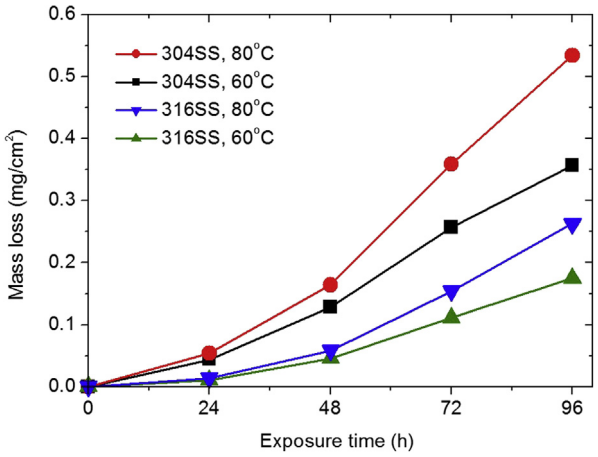

Fig. 2. Mass loss versus exposure time for 304SS and 316SS.

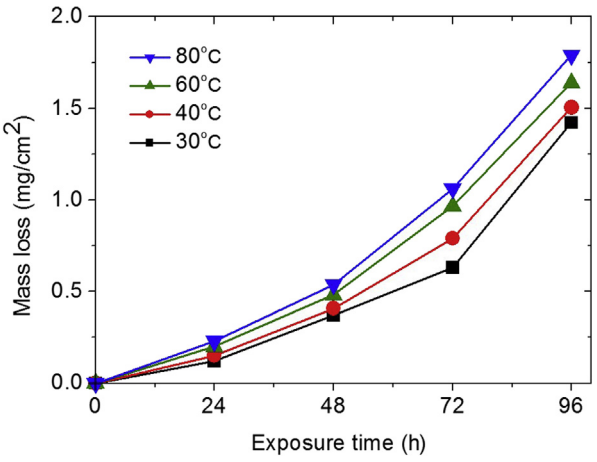

Fig. 3. Mass loss versus exposure time for copper.

hours, 72 hours, and 96 hours, respectively. The weight loss of 316SS was about half that of 304SS, because its Mo content forms a strong metallic compound (Mo-Cr-Ni) on the surface that provides corrosion resistance better than that of 304SS [19].

The corrosion of copper was accelerated by LiCl-KCl at all temperatures and, much as in the case of stainless steel, the weight loss increased more swiftly as the temperature increased. As can be seen in Fig. 3, the weight loss of 0.1–0.2 mg/cm^2 after 24 hours gradually increased with time to 1.3–1.7 mg/cm^2 after 96 hours. Considering that the weight loss of copper was about three times higher than that of stainless steel, it would seem that copper is more vulnerable to corrosion induced by chloride ions.

3.2. Surface analysis

Fig. 4 shows the corrosion of each specimen at each temperature after 96 hours. In the case of stainless steel, almost no corrosion was observed at 30°C, but a brown corrosion product appeared at temperatures above 40°C. Above 60°C, small circular holes formed at the boundaries of the specimen, with corrosion products being generated around them. This is consistent with the pitting corrosion often observed in stainless steel. By comparing these results with the weight loss data, we can see that the rate of corrosion rapidly accelerates at temperatures above 60°C. This can be further confirmed by the SEM results shown in Figs. 5A and 5B, which show that there is almost no corrosion product on either type of stainless steel at 30°C. By contrast, a number of small corrosion product particles were found on both the 304SS and 316SS samples at 60°C (Figs. 5C and 5D). Figs. 5E and 5F show the areas in which pitting corrosion occurred at 60°C, revealing that numerous corrosion products formed to create a kind of layer.

The corrosion products formed at 30°C for copper were difficult to discern due to their very small quantity, but increased as the temperature increased. At 80°C, the corrosion products increased to a visible level (Fig. 4). The mode of corrosion here was unlike that of stainless steel, as corrosion occurred over the entire surface of the specimen and can be defined as general corrosion. This is seemingly the reason that the weight loss of copper is about three times higher than that of stainless steel. Fig. 6 shows 500× magnified SEM images of the surface of the copper sample at 30°C and 60°C after 24 hours and 72 hours. This reveals that although almost no corrosion products are generated after 24 hours at 30°C, 10 μm-sized corrosion product particles are sporadically formed at 60°C (Figs. 6A and 6C). After 72 hours, numerous corrosion product particles were observed at both 30°C and 60°C, with those

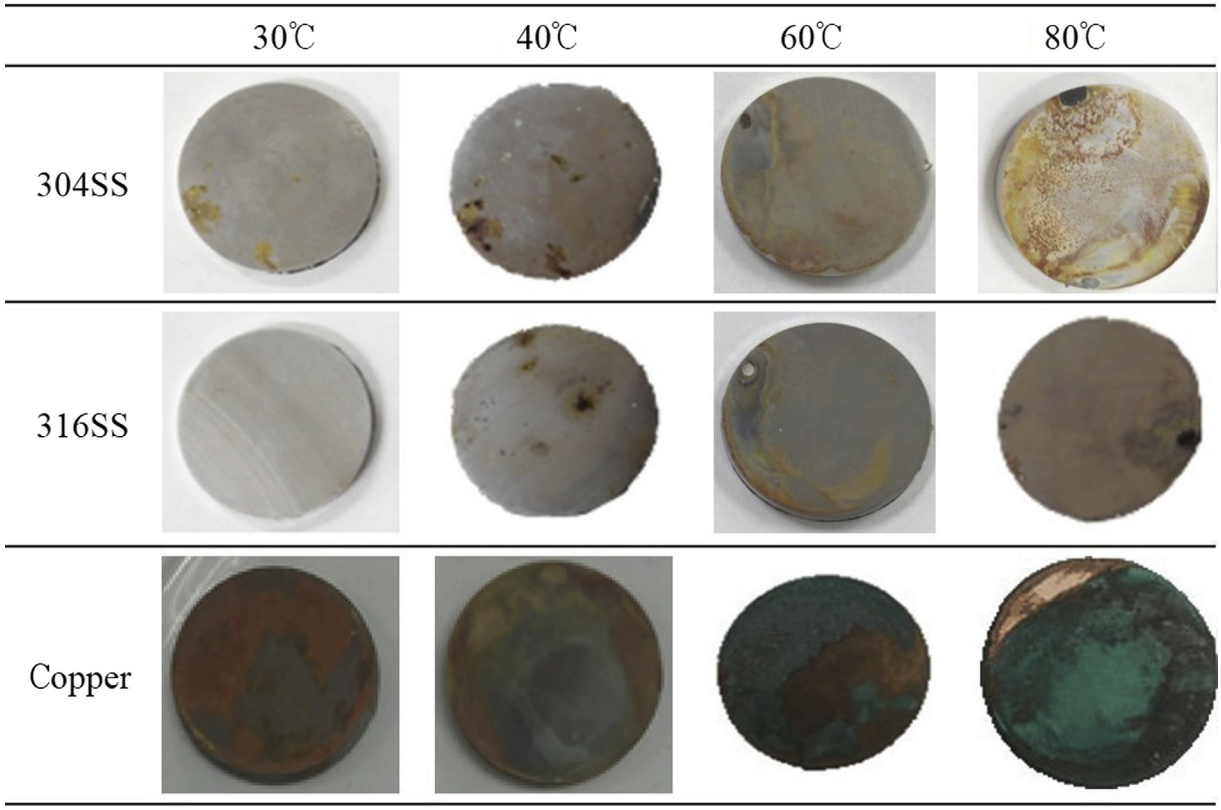

Fig. 4. Surface of specimens after 96 hours of corrosion.

produced at 30°C being small in size (< 10 μm) and overlapped to form a kind of corrosion product layer (Fig. 6B). At 60°C, a thicker and more distinct corrosion product layer formed across the entire surface (Fig. 6D). According to Gu et al [20], a CuCl coating is primarily formed on the surface of copper that is in a medium including chloride ions. However, as the corrosion resistance of copper is low, this reaction continues and ultimately forms $CuCl_2$ as the corrosion product. This same reaction appears to have taken place in the present study.

3.3. Corrosion product analysis

The corrosion products were analyzed by AES and XPS to determine their composition and chemical states. The AES results for the 304SS sample corroded for 24 hours at 60°C reveal an oxidation thickness of about 30 nm (Fig. 7A); the concentrations of iron and chromium are nearly 0 at the surface, but increase with depth. This indicates that the oxides formed mainly consist of iron and chromium. The potassium concentration rose by about 20%, and then rapidly decreased, whereas the chlorine concentration was as low as a few percent at the surface and it was almost not included in the oxides. After 72 hours, the concentrations of the major components exhibited a similar trend, but the thickness of the oxide layer increased to about 100 nm (Fig. 7B). The 316SS sample exhibited a similar change in the concentration of its components at depth, but the thicknesses of the oxides were only 15 nm and 70 nm after 24 hours and 72 hours, respectively (Figs. 8A and 8B). The XPS analysis results showed that the major corrosion products of 304SS were Cr_2O_3, Ni_2O_3, Fe_2O_3, and Fe_3O_4; 316SS was similar expect for the addition of Mo oxides (Fig. 9, Table 2).

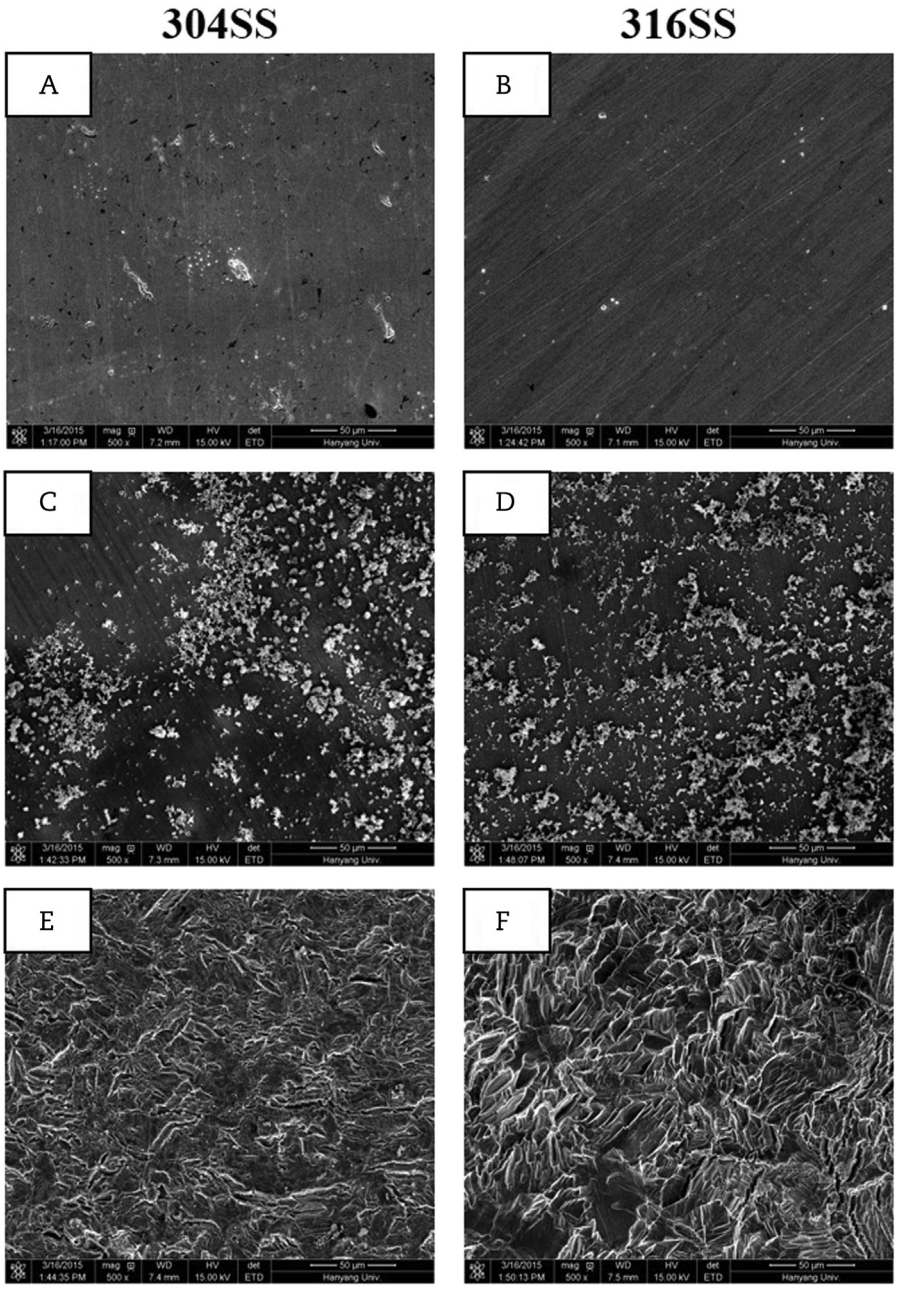

Fig. 5. SEM images (500× magnification) of stainless steel samples corroded at (A) 304SS, 30°C (B) 316SS, 30°C (C, E) 304SS, 60°C and (D, F) 316SS, 60°C for 72 hours.

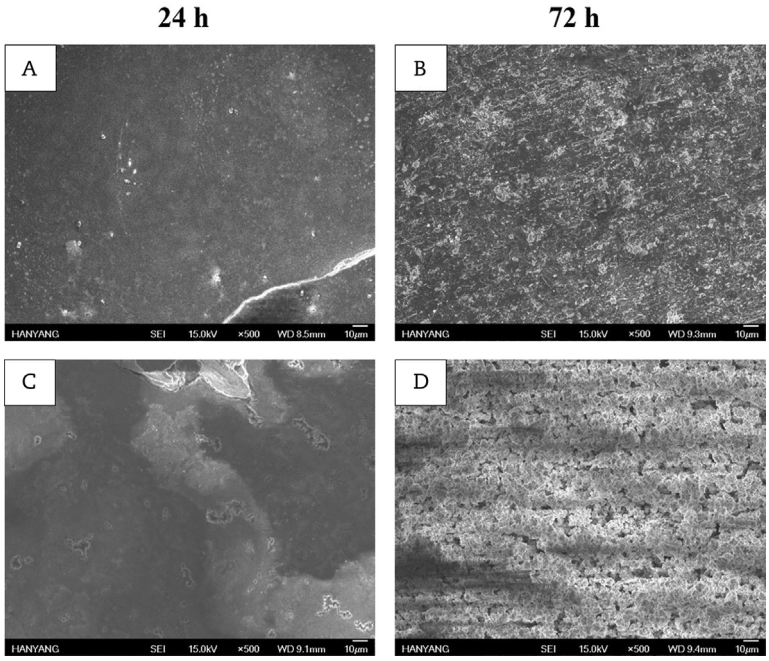

Fig. 6. SEM images (500× magnification) of copper samples corroded at (A) 30°C, 24 hours (B) 30°C, 72 hours (C) 60°C, 24 hours and (D) 60°C, 72 hours.

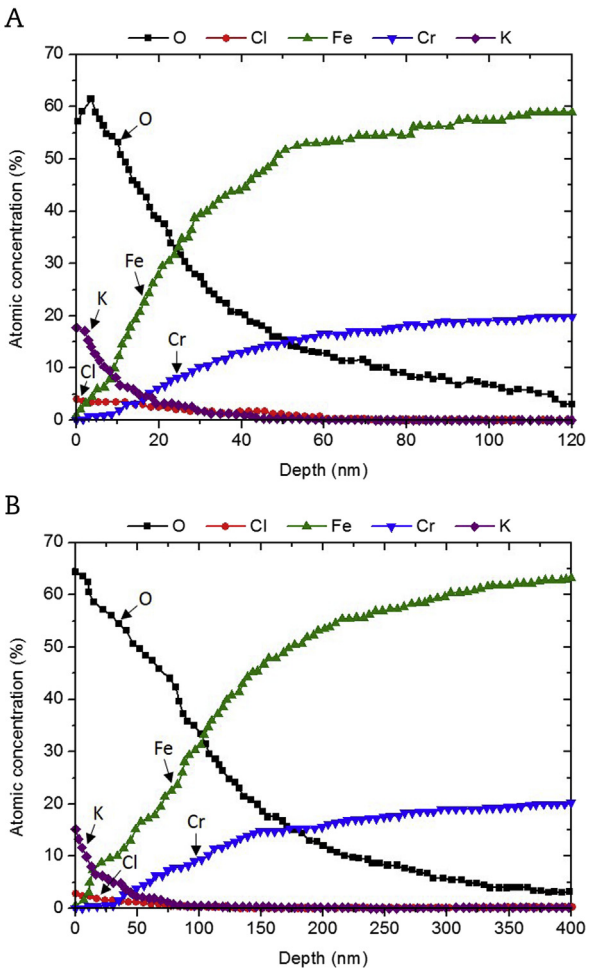

Fig. 7. AES depth profiling for 304SS corroded at (A) 60°C, 24 hours and (B) 60°C, 72 hours.

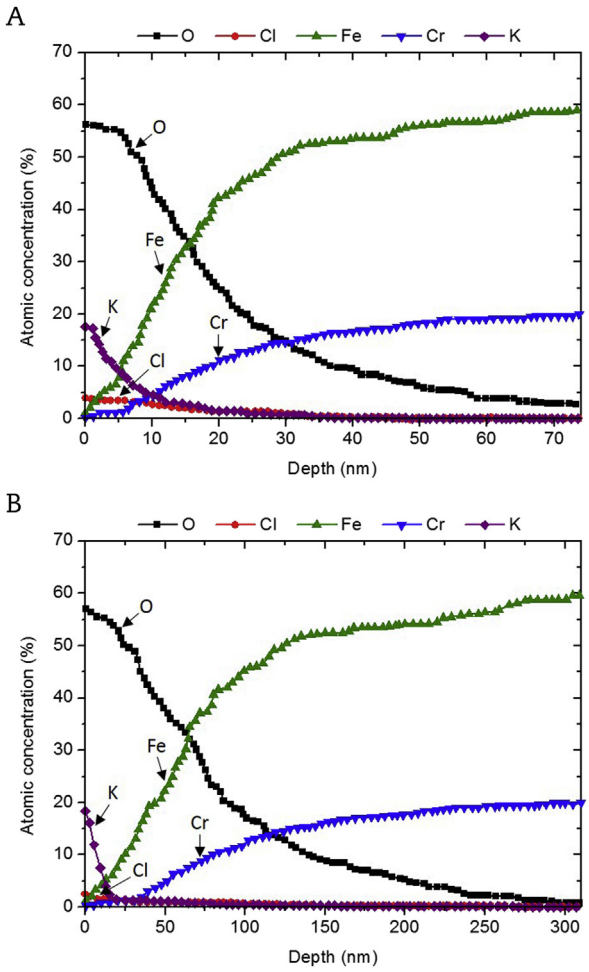

Fig. 8. AES depth profiling for 316SS corroded at (A) 60°C, 24 hours and (B) 60°C, 72 hours.

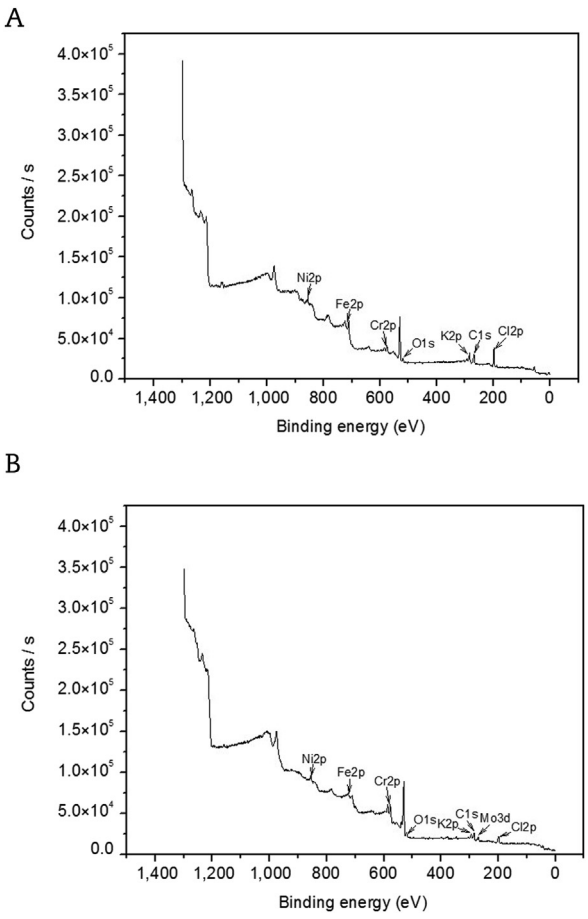

Fig. 9. XPS spectra for stainless steel samples corroded at 60°C for 72 hours. (A) 304SS and (B) 316SS.

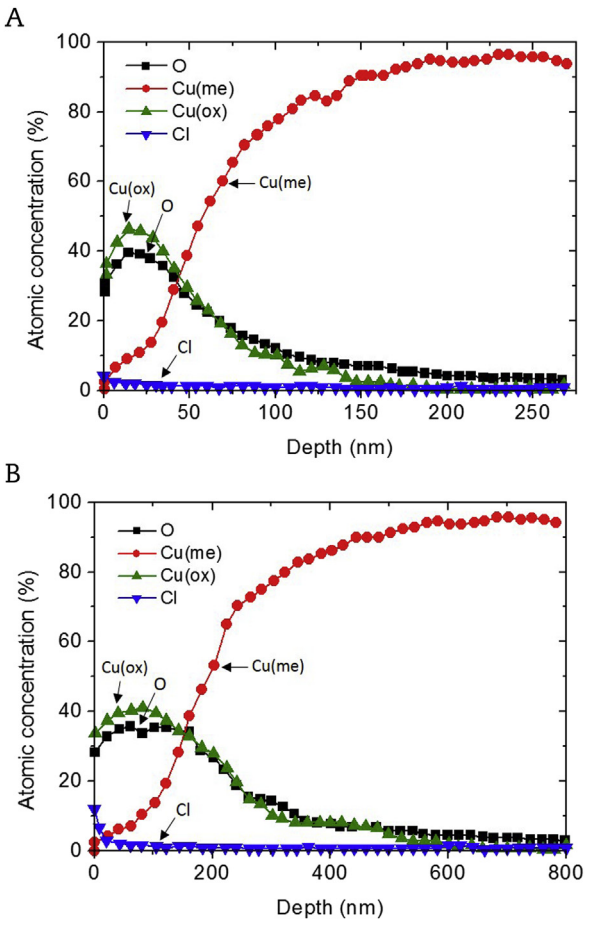

Fig. 10. AES depth profiling for copper corroded at (A) 60°C, 24 hours and (B) 60°C, 72 hours.

According to the study on the corrosion of Fe-Cr alloy, oxide layers with high chromium content act as passive films, thus granting the surface good corrosion resistance [15,21]. However, this passive film is locally destroyed in an environment that includes chloride ions, which allows corrosion to occur. According to Pettersson et al [21], chromium oxide layers with high corrosion resistance can also turn into a potassium chromate layer with low corrosion resistance via the following reaction [21]:

$$(Cr_{1-x},\ Fe_x)_2O_3(s) + 4KCl(s) + 2H_2O(g) + (3/2)O_2(g) \rightarrow xFe_xO_3(s) + 2(1-x)K_2CrO_4(s) + 4HCl(g)$$

Based on the surface and composition analysis results, this appears to be the same process of corrosion that occurred in the present experiment.

Table 2
XPS results of stainless steel corroded samples.

Element	Peak binding energy (eV)		Associated compound
	304SS	316SS	
C1s	284.51	284.61	—
O1s	530.76	531.32	—
K2p	292.95	293.74	—
Cl2p	198.31	198.76	—
Cr2p	576.36	577.00	Cr_2O_3
Fe2p	711.11	711.22	Fe_2O_3, Fe_3O_4
Ni2p	855.39	855.72	Ni_2O_3
Mo3d	—	232.40	Mo_2O_3

In the case of copper, the AES analysis results indicated that a 50 nm-thick layer of copper oxide was formed after 24 hours, and that this layer increased in thickness to about 200 nm after 72 hours (Fig. 10). Moreover, the concentration of Cl ions near the surface was about 10 at.%. Subsequent XPS analysis confirmed that the corrosion products were Cu_2O and $CuCl_2$ (Fig. 11, Table 3). According to Chon and Kim [22], the oxidation of copper in a medium containing chloride ions, oxygen, and moisture produces $CuCl_2$, and is heavily influenced by the chloride ion concentration, whereas the

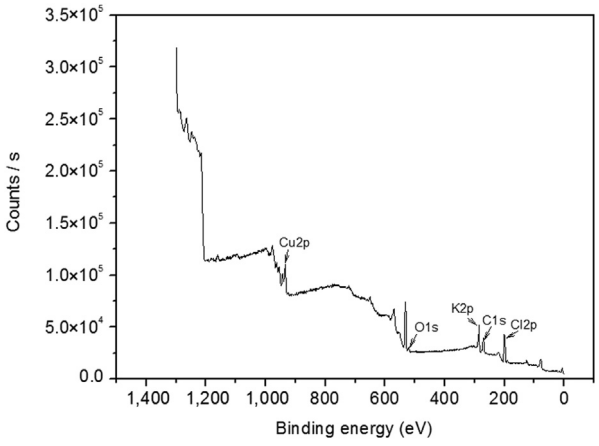

Fig. 11. XPS spectra for copper sample corroded at 60°C for 72 hours.

Table 3
XPS results of copper corroded samples.

Element	Peak binding energy (eV)	Associated compound
C1s	285.01	—
O1s	531.20	Cu_2O
K2p	293.92	—
Cl2p	198.72	$CuCl_2$
Cu2p	932.62	Cu bulk

formation of Cu_2O is triggered by the presence of OH^-. These two reactions are mutually competitive, depending on the oxygen concentration. Consequently, even though it was not possible in this experiment to determine which of the two reactions was dominant, it can at least be inferred that both occurred.

4. Conclusion

This investigation into the corrosion of 304SS, 316SS and copper induced by LiCl-KCl in an environment with sufficient oxygen and moisture has confirmed that localized corrosion of stainless steel caused by the destruction of its passive film by chloride ions occurs at temperatures above 60°C. In the case of copper, accelerated corrosion rates were found regardless of the temperature, and so even at low temperatures of 30–80°C, the presence of LiCl-KCl can have a significant, long-term impact on the major structural materials of PRIDE. It is therefore important to minimize the moisture and oxygen levels to ensure the integrity and stability of the facility.

Conflicts of interest

The authors declare no conflicts of interest.

Acknowledgments

This work was supported by the Research and Development Program of the Korea Atomic Energy Research Institute (KAERI), through a grant funded by the Korean Government (Ministry of Science, SCT and Future Planning).

References

[1] H.S. Lee, et al., Korea Atomic Energy Research Institute (KAERI) report, Development of Volume Reduction Technology for PWR Spent Fuel by Pyroprocessing, KAERI/RR-3400/2011, Korea, 2012.
[2] Y.I. Chang, The integral fast reactor, Nucl. Technol. 88 (1989) 129–138.
[3] T. Inoue, Actinide recycling by pyro-process with metal fuel FBR for future nuclear fuel cycle system, Prog. Nucl. Energy 40 (2002) 547–554.
[4] M. Iizuka, K. Kinoshita, Y. Sakamura, T. Ogata, T. Koyama, Performance of pyroprocess equipment of semi-industrial design and material balance in repeated oxide/metal fuels, Nucl. Technol. 184 (2013) 107–120.
[5] H.S. Lee, G.I. Park, K.H. Kang, J.M. Hur, J.G. Kim, D.H. Ahn, Y.Z. Cho, E.H. Kim, Pyroprocessing technology development at KAERI, Nucl. Eng. Technol. 43 (2011) 317–328.
[6] G.S. You, I.J. Cho, W.M. Choung, E.P. Lee, D.H. Hong, W.K. Lee, J.H. Ku, Concept and safety studies of an integrated pyroprocess facility, Nucl. Eng. Des. 241 (2011) 415–424.
[7] Y. Shinata, F. Takahashi, K. Hashiura, NaCl-induced hot corrosion of stainless steels, Mater. Sci. Eng. 87 (1987) 399–405.
[8] T. Raghu, S.N. Malhotra, P. Ramakrishnan, Corrosion behavior of porous sintered type 316L austenitic stainless steel in 3% NaCl solution, Corrosion 45 (1989) 698–704.
[9] A.U. Malik, P.C. Mayan Kutty, N.A. Siddiqi, I.N. Andijani, S. Ahmed, The influence of pH and chloride concentration on the corrosion behavior of AISI 316L steel in aqueous solutions, Corros. Sci. 33 (1992) 1809–1827.
[10] E. Otero, A. Pardo, M.V. Utrilla, E. Sáenz, F.J. Perez, Influence of microstructure on the corrosion resistance of AISI Type 304L and Type 316L sintered stainless steels exposed to ferric chloride solutions, Mater. Charact. 35 (1995) 145–151.
[11] J.E. Indacochea, J.L. Smith, K.R. Litko, E.J. Karell, Corrosion performance of ferrous and refractory metals in molten salts under reducing conditions, J. Mater. Res. 14 (1999) 1990–1995.
[12] A.R. Shankar, U.K. Mudali, Corrosion of type 316L stainless steel in molten LiCl-KCl salt, Mater. Corros. 59 (2008) 878–882.
[13] A.K. Singh, V. Chaudhary, A. Sharma, Electrochemical studies of stainless steel corrosion in peroxide solutions, Port. Electrochim. Acta 30 (2012) 99–109.
[14] G. Kear, B.D. Barker, F.C. Walsh, Electrochemical corrosion of unalloyed copper in chloride media-A critical review, Corros. Sci. 16 (2004) 109–135.
[15] J. Pettersson, J.-E. Svensson, L.-G. Johansson, KCl-induced corrosion of a 304-type austenitic stainless steel in O_2 and in O_2+H_2O environment: The influence of temperature, Oxid. Met. 72 (2009) 159–177.
[16] U. Berocci, An EQMB examination of Cu surface oxides in borate buffer, Electrochim. Acta 49 (2004) 1831–1841.
[17] H.P. Lee, K. Nobe, Film formation and current oscillations in the electrodissolution of Cu in acidic chloride media, J. Electrochem. Soc. 132 (1985) 1031–1037.
[18] KS D ISO 8407, Corrosion of metals and alloys – Removal of corrosion products from corrosion test specimens, Korean Standards Association, 2014.
[19] I. Sekine, A. Masuko, K. Senoo, Corrosion behavior of AISI 316 stainless steel in formic and acetic acid solutions, Corrosion 43 (1987) 553–560.
[20] Z.H. Gu, S.J. Xiz, T.Z. Fahidy, Comparison of dynamic behaviour of the anodic dissolution of copper in aqueous chloride and bromide solutions, Electrochim. Acta 14 (1996) 2045–2054.
[21] J. Pettersson, H. Asteman, J.-E. Svensson, L.-G. Johansson, KCl Induced corrosion of a 304-type austenitic stainless steel at 600°C, The role of potassium, Oxid. Met. 64 (2005) 23–41.
[22] J.K. Chon, Y.K. Kim, Corrosion and passivation of copper in artificial sea water, J. Korean Chem. Soc. 51 (2007) 305–311.